Eur. Phys. J. AP **6**, 71–79 (1999)

THE EUROPEAN PHYSICAL JOURNAL APPLIED PHYSICS

Analytical modelling of travelling-wave piezomotor stators using a variational approach

C. Giraud-Audine[a] and B. Nogarède[b]

Laboratoire d'Électrotechnique et d'Électronique Industrielle[c], 2 rue Camichel, 31071 Toulouse, France

Received: 23 June 1998 / Revised: 7 December 1998 / Accepted: 6 January 1999

Abstract. This article deals with a general method for finding the equations of the dynamic response of a bimorphous piezoelectric structure through a variational formulation. First, a method of resolution is proposed then a general electric equivalent circuit involving the design parameters of the device is deduced, followed by the description of application to a travelling-wave stator.

PACS. 43.38.Fx Piezoelectric and ferroelectric transducers – 43.40.Dx Vibrations of membrane and plates – 77.65.-j Piezoelectricity and electrostriction

1 Introduction

Among the new principles of electromechanical energy conversion currently explored, actuators based on the piezoelectric phenomenon are some of the most promising. However, the complex reactive load of these actuators, together with the high levels of voltages and frequencies needed by the transducer, results in motors requiring specific power supplies.

In this respect, the approach through equivalent circuits has already proved interesting and efficient, but so far it relies on the identification of the parameters of an existing actuator [1,2]. In order to reach an optimized design of a power supply together with its actuator, it seems interesting to develop methods which allow *a priori* characterization, starting from the sole knowledge of the geometric parameters and the characterization of the electroactive materials.

With this in view, a general method of analysis based on the use of variational principles is presented. The method developed is used to predict the electromechanical behaviour of a classical piezoelectric bimorph structure. After obtaining the general Lagrangian expression of a piezoelectric device, the equations of a thin bimorph plate are derived from Hamilton's principle, then a general method of resolution is presented. Finally the model obtained will be applied and validated by considering the case of an annular piezoelectric travelling-wave motor stator.

[a] e-mail: giraud@leei.enseeiht.fr
[b] e-mail: nogarede@leei.enseeiht.fr
[c] URA 5828 CNRS

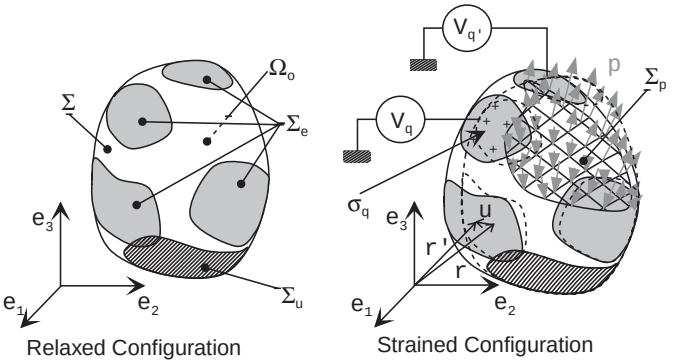

Fig. 1. Schema of a general electro-elastically coupled problem.

2 Formulation of the electroelastic coupled problem

The originality of the electromechanical conversion occurring within a piezoelectric device is due to local coupling between electrostatic and elastic phenomena. It is therefore necessary to take an approach whereby the global behaviour of a structure from a local description of the phenomenon can be deduced. Hamilton's principle will therefore be applied to find the equation of such problems [4]. The general problem of an electroelastic coupled problem is to determine mechanical and electrical values *i.e.* the displacement field $\mathbf{u}$, the stress tensor $\mathbf{T}$, the electric field $\mathbf{E}$ and the electric displacement field $\mathbf{D}$ in a body occupying a volume Ω. The domain Ω is bounded by the surface Σ which can be subdivided as shown in Figure 1 according to the type of conditions applied. Those subsurfaces will be designated as follows:

– Σ_e: electroded surfaces;

– Σ_{u}: kinematically constrained surfaces;
– $\Sigma_{\mathrm{p}} = \Sigma/\Sigma_{\mathrm{u}}$: mechanically loaded surfaces.

The fundamental step is to establish the Lagrange function L of the device under study which involves the general coordinates q_i and the generalized impulses p_i of the system by [5]:

$$\mathrm{d}L = \dot{p}_i \mathrm{d}q_i + p_i \mathrm{d}\dot{q}_i. \tag{1}$$

The mechanical aspect of the solution to the problem goes *via* the determination of $u(x_i, t)$ which is the shift between the relaxed configuration and the strained configuration of the system. In the hypothesis of small strains and small displacement, the strain tensor $\mathbf{S}$ is deduced $\mathbf{u}(x_i, t)$ from the relations[1] [7]:

$$S_{ij} = \frac{1}{2}\left(u_{i,j} + u_{j,i}\right) \quad i, j \in \{1, 2, 3\}. \tag{2}$$

Those components constitute the mechanical coordinates, while $\rho\dot{\mathbf{u}}$ constitutes the generalized volumic impulses. The strains in the deformed body generate stresses which tend to bring it back to its former state. The stress tensor $\mathbf{T}$ is related to the stress tensor component[2] by relations depending on the nature of the material, as we shall see later.

Some ambiguity remains concerning the electrical aspect, since it is possible to assimilate the electric displacement field $\mathbf{D}$ to a generalized coordinate, or a generalized impulse [6]. By making the second choice, the total differential form of the Lagrangian of an electroelastic coupled problem will be, taking (1):

$$\mathrm{d}L(\mathbf{S}, \mathbf{E}, \dot{\mathbf{u}}) = \mathbf{D}\mathrm{d}\mathbf{E} + \rho\dot{\mathbf{u}}\mathrm{d}\dot{\mathbf{u}} - \mathbf{T}\mathrm{d}\mathbf{S}. \tag{3}$$

$\mathbf{D}$ and $\mathbf{T}$ must then be linked with the independent variables thus defined: $\mathbf{S}$ and $\mathbf{E}$. This is achieved through the constitutive laws of the behavior of piezoelectric media [3]:

$$T_i = c^{\mathrm{E}}_{ij} S_j + e_{mi} E_m \tag{4a}$$

$$D_n = e_{nj} S_j + \epsilon^{\mathrm{S}}_{nm} E_m \tag{4b}$$

$$\text{where } i, j = \{1, \ldots, 6\} \text{ and } m, n = \{1, \ldots, 3\}$$

in which coefficient c^{E}_{ij}, $\epsilon^{\mathrm{S}}_{nm}$ et e_{nj} represent respectively constant electric field compliances, constant strain permittivity and piezoelectric constants.

Formula (3) corresponds to an autonomous system, and it must be complemented by taking into account both the densities of mechanical load applied on the portion of boundary Σ_{p} and the action of the generators on the electroded region Σ_{e}. Let $\mathbf{p}$ be the distribution of mechanical load on Σ_{p} (on parts of Σ_{p} where no load is applied, $\mathbf{p}$ will be equal to zero). The working of the generators, which intervenes in the Lagrangian expression as a kinetic coenergy, can be written for the qth electrode, provided that, due to our previous choice, the electric potential Φ is a general coordinate and the local electric load σ (C/m^2) a force:

$$\delta W_q = Q_q \delta V_q = \left(\int_{\Sigma_{e_q}} \sigma_q \mathrm{d}\Sigma_{e_q} \right) \delta V_q \tag{5}$$

where Q_q is the total electric load provided by generator q, and V_q its voltage. As for mechanical load, we can consider a single distribution σ which will be equal to σ_q on the convenient surfaces and nil on $\Sigma/\Sigma_{\mathrm{e}}$. Considering that $\mathbf{p}$ and V_q are imposed time dependent variables, the Lagrangian then becomes:

$$\begin{aligned} L = \frac{1}{2}\int_\Omega \rho\dot{u}_k\dot{u}_k + \epsilon^S_{nm}E_nE_m + 2e_{nj}E_nS_j - c^{\mathrm{E}}_{ij}S_iS_j \mathrm{d}\Omega \\ - \int_{\Sigma_m} f_k u_k \mathrm{d}\Sigma - \sum_{q=1}^{n_{\mathrm{e}}} \int_{\Sigma_{e_q}} \sigma V_q \mathrm{d}\Sigma_{e_q} \\ i, j \in \{1, \ldots, 6\}, \ k, l, m \in \{1, 2, 3\} \text{ and } n_{\mathrm{e}} \in \mathbb{N}. \end{aligned} \tag{6}$$

The application of Hamilton's principle to expression (6) then makes it possible to find the equations of equilibrium in volume Ω of the body as well as boundary conditions along its frontier Σ. When including electrical potential Φ linked to the electrical field in the electrostatic hypothesis through the relation:

$$\mathbf{E} = -\mathrm{grad}\Phi \tag{7}$$

calculation of the variation of the Action [4] gives:

$$\begin{aligned} \delta A &= \int_{t_1}^{t_2} \delta L \mathrm{d}t \Rightarrow \\ \delta A &= \int_{t_1}^{t_2} \left(\int_\Omega \left\{ \mathrm{div}(\mathbf{T}) - \rho\ddot{\mathbf{u}} \right\} \delta\mathbf{u} - \left\{ \mathrm{div}(\mathbf{D}) \right\} \delta\Phi \mathrm{d}\Omega \right. \\ &\quad \left. - \int_\Sigma \left\{ \mathbf{T}\cdot\mathbf{n} - \mathbf{f} \right\} \delta\mathbf{u} + \left\{ \mathbf{D}\cdot\mathbf{n} - \sigma \right\} \delta\Phi \mathrm{d}\Sigma \right) \mathrm{d}t. \end{aligned} \tag{8}$$

Now $\delta A = 0$ for any variation of the coordinates, can only be validated within the volume if the terms in brackets are equal to zero. On the surface the same conclusion is true for the sub-domains of the boundary for which the coordinates are not constrained. Should they be constrained, there are no variations. The equations of equilibrium in the volume Ω thus obtained are:

$$\begin{cases} \left(c^{\mathrm{E}}_{ij} S_j + e_{jm} E_m \right)_{,i} = \rho\ddot{u}_i \\ \left(e_{nj} S_j + \epsilon^{\mathrm{S}}_{nm} E_m \right)_{,n} = 0 \end{cases} \tag{9}$$

with boundary-conditions:

$$\begin{cases} \left(c^{\mathrm{E}}_{ij} S_j + e_{mj} E_m \right) n_i = f_i \quad \text{on } \Sigma_{\mathrm{p}} \\ \qquad\qquad \text{or } \delta\mathbf{u} = 0 \quad \text{on } \Sigma_{\mathrm{u}} \\ \left(e_{nj} S_j + \epsilon^{\mathrm{S}}_{nm} E_m \right) n_n = \sigma \quad \text{on } \Sigma \\ \qquad\qquad \text{or } \delta\Phi = 0 \quad \text{on } \Sigma_{\mathrm{e}} \end{cases}. \tag{10}$$

[1] We shall use the summation on repeated subscript, and note f_i the derivation in the $\mathbf{e}_i$ direction of a function f.

[2] The stress and strain tensors being symmetrical, they therefore contain only 6 independent components. In order to simplify the index notation, we shall use the "engineering" notations which substitute 6 dimension vectors to the second order tensors from this point.

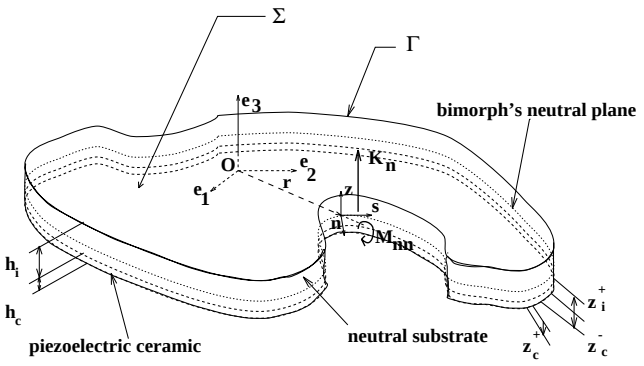

Fig. 2. Scheme of a thin piezoelectric bimorph structure.

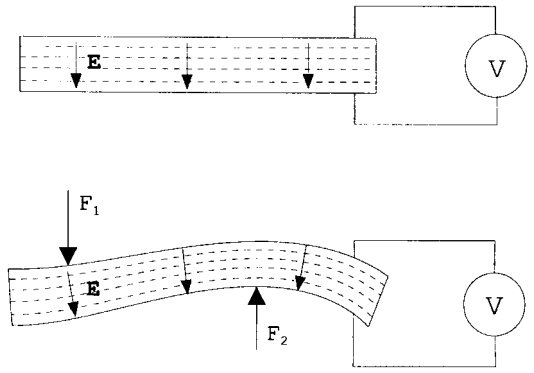

Fig. 3. Model of the evolution of the electric field during deformations.

Having reached this stage, the exact electroelastic problem is fully formulated in terms of partial derivatives with conditions on the boundaries. In most cases the solution to the problem will rely on numerical methods such as finite elements methods. The purpose of the proposed method, however, is to use the variational principles as a systematic tool to formulate both local equations and boundary conditions, within the context of approximations of the real fields.

3 Modelization of a flexed bimorph piezoelectric structure

One particularly interesting case is the one in which one dimension of the piezoelectric environment is negligible in relation to the others. This configuration is often used in the case of a bimorph device, the structure of which is presented in Figure 2. It consists in the superposition of thin layers of active and passive materials to obtain bending deformations as in travelling-wave motors or active diaphragms in micro-pumps. The thinness of those devices in relation to their surface allows for a number of simplifications as to the different fields involved.

3.1 Simplifying assumptions

From now on we shall be more particularly concerned with flat cylindrical bimorphous structures. The boundary of the latter is designated by Γ limiting the surface Σ. We suppose that the potentials are imposed on the entire surface of Σ, and consider the case of a transverse coupling. The bimorph is marked by a Cartesian referential $\mathcal{R}\{O, \mathbf{e}_1, \mathbf{e}_2, \mathbf{e}_3\}$ so that $\mathbf{e}_3$ is orientated in a parallel fashion to the polarization direction along the thickness, *i.e.* perpendicular to the surface of the bimorph, plane $O, \mathbf{e}_1, \mathbf{e}_2$ containing the neutral plane (Fig. 2). When the bimorph bends, the convex part is submitted to compression, and the concave part to traction, while inside the bimorph, there is a so-called neutral surface in which stresses vanish. Let w be the displacement in direction $\mathbf{e}_3$, of points of the neutral surface. As the bimorph is thin, the forces required to bend it are weak in relation to the stress due to the traction and compression of the fibers. We may thus infer that:

$$\begin{cases} T_3 = 0 \\ T_4 = 0 \\ T_5 = 0 \end{cases}. \tag{11}$$

Moreover, from the electric point of view, in the case of completely electroded ceramics, the ceramics are supposed to behave like a condenser with a parallel framework. We shall then suppose that the electrical equipotentials are "parallel" to the electrodes during deformation (Fig. 3). Thus if V_0 is the voltage applied to the electrodes of the ceramics, the electric potential Φ will be (considering a polynomial approximation to the first order):

$$\Phi = \frac{V_0}{h_c}\left(w(x_1, x_2) + x_3\right) \tag{12}$$

where h_c is the thickness of the ceramic layer as shown in Figure 2. However, as the curve is big, its influence may reasonably be neglected and the electric field may be modelled as follows:

$$\mathbf{E} = \begin{Bmatrix} 0 \\ 0 \\ -V_0/h_c \end{Bmatrix}. \tag{13}$$

Back to the mechanical aspect, it can be shown that conditions (11, 2, 4a) and the previous model of the electric field, impose the following displacement field:

$$\mathbf{u} = \begin{Bmatrix} -x_3 w(x_1, x_2)_{,1} \\ -x_3 w(x_1, x_2)_{,2} \\ w(x_1, x_2) \end{Bmatrix}. \tag{14}$$

Kinematically, the approximation which has been adopted means that we consider that a segment orthogonal to the neutral plane remains straight and perpendicular to the neutral surface during flexure. The latter kinematical

constraint results from the fact that the shearing stress around $\mathbf{e}_1$ and $\mathbf{e}_2$ are neglected. Moreover, no distinction is made between the displacement fields in relation to the substrate. This implicitly supposes that cohesion is perfect, *i.e.* that there is no relative slipping between the two fields. The position of the neutral plane remains to be determined to allow a complete definition of the displacement field. However, in order to model the flexion of the bimorph, the average stress on the thickness will be zero when no voltage is applied. Therefore, the expression of the stress components must now be established.

3.2 Expressions of the stresses

Given (14), the tensor of strains is defined by three components. Adopting the engineering notation of component, we have [8]:

$$\begin{cases} S_1 = -x_3 w(x_1, x_2)_{,11} \\ S_2 = -x_3 w(x_1, x_2)_{,22} \\ S_6 = -x_3 w(x_1, x_2)_{,12} \end{cases}. \tag{15}$$

According to (11), the material characteristics have to be calculated under those stress conditions. This can be achieved by replacing the (11) conditions into the constitutive piezoelectric equations expressed with the intensive variables set $(\mathbf{T}, \mathbf{E})$. Then the inverse characteristic matrix gives the "plate" rigidities ($c^{\mathrm{E}}_{11_{\mathrm{p}}}$, $c^{\mathrm{E}}_{12_{\mathrm{p}}}$, $c^{\mathrm{E}}_{66_{\mathrm{p}}}$), permittivity $\varepsilon^{\mathrm{E}}_{33_{\mathrm{p}}}$ and piezoelectric constant $e_{13_{\mathrm{p}}}$. Moreover a distinction has to be made depending on the substrate. Given equations (15, 13) the field of stress in the piezoelectric ceramic is expressed by:

$$\begin{cases} T_{1_{\mathrm{c}}} = \mathcal{C}^{\mathrm{E}}_{11_{\mathrm{p}}} S_1 + \mathcal{C}^{\mathrm{E}}_{12_{\mathrm{p}}} S_2 - e_{13_{\mathrm{p}}} E_3 \\ T_{2_{\mathrm{c}}} = \mathcal{C}^{\mathrm{E}}_{12_{\mathrm{p}}} S_1 + \mathcal{C}^{\mathrm{E}}_{11_{\mathrm{p}}} S_2 - e_{13_{\mathrm{p}}} E_3 \\ T_{6_{\mathrm{c}}} = \mathcal{C}^{\mathrm{E}}_{66_{\mathrm{p}}} S_6 \end{cases}. \tag{16}$$

On the other hand, the neutral material is supposed to be isotropic. Stresses are then expressed by the following relations (once again with material characteristics adaptated to the "plate" stress conditions):

$$\begin{cases} T_{1_i} = \dfrac{E}{1-\nu^2}(S_1 + \nu S_2) \\ T_{2_i} = \dfrac{E}{1-\nu^2}(\nu S_1 + S_2) \\ T_{6_i} = \dfrac{E}{1+\nu} S_6 \end{cases}. \tag{17}$$

Let the origin O of referential $\mathcal{R}$ be in the bimorph neutral plane, and let us introduce a non-dimensional parameter α so that the height z_n of the mirror plane of the neutral material thickness is given by:

$$z_n = -\alpha \frac{h_i + h_{\mathrm{c}}}{2} \tag{18}$$

in which h_i and h_{c} are the respective thicknesses of the neutral material and the ceramic (*cf.* Fig. 2). The different stresses being defined, we can now calculate the α parameter, and hence completely model the mechanical fields. Applying the flexion stress field condition, we have:

$$\alpha = \frac{-\left(c^{\mathrm{E}}_{11_{\mathrm{p}}} + c^{\mathrm{E}}_{12_{\mathrm{p}}}\right) h_{\mathrm{c}}}{\left(c^{\mathrm{E}}_{11_{\mathrm{p}}} + c^{\mathrm{E}}_{12_{\mathrm{p}}}\right) h_{\mathrm{c}} + \frac{E}{1-\nu} h_i}. \tag{19}$$

Actually, when a voltage is applied to the bimorph structure, the mean value of the stress along the thickness is no longer equal to zero; then a traction displacement field in the plane of the plate appears. However, if the traction and flexion modes are not coupled, we can assume that the traction field occurs under quasi-static conditions, therefore, it will be neglected compared with the flexure displacement field.

As for the field of electric displacement $\mathbf{D}$, since there are no strains due to shearing in the planes containing $\mathbf{e}_3$, and as the components of the electric field $\mathbf{E}$ orthogonal to that same direction are equally neglected, one component only will not be equal to zero:

$$D_3 = e_{13_{\mathrm{p}}}(S_1 + S_2) + \epsilon^{\mathrm{S}}_{33_{\mathrm{p}}} E_3. \tag{20}$$

3.3 Equations of a piezoelectric bimorph structure

3.3.1 Expression of the Lagrangian

Let us then express the Lagrangian of the bimorph, which now includes two specific fields induced by (16, 17):

$$\begin{aligned} L = \frac{1}{2}\int_{\Sigma} \Bigg(\int_{z_{\mathrm{c}}^-}^{z_{\mathrm{c}}^+} & (D_3 E_3 + \rho_{\mathrm{c}} \dot{\mathbf{u}} \cdot \dot{\mathbf{u}} - T_{1_{\mathrm{c}}} S_1 - T_{2_{\mathrm{c}}} S_2 \\ & - T_{6_{\mathrm{c}}} S_6) \mathrm{d}x_3 + \int_{z_{\mathrm{c}}^+}^{z_i^+} (\rho_i \dot{\mathbf{u}} \cdot \dot{\mathbf{u}} - T_{1_i} S_1 - T_{2_i} S_2 \\ & - T_{6_i} S_6) \mathrm{d}x_3 \Bigg) \mathrm{d}\Sigma. \end{aligned} \tag{21}$$

Variable x_3 intervenes only as a factor of function w. Thus, it is possible to perform the integration along the thickness, and to introduce the reducing elements of the bimorph: its mass per surface unit M_{b} and its flexural rigidity per surface unit D_{b} respectively calculated from formulas (22, 23)

$$M_{\mathrm{b}} = \rho_{\mathrm{c}} h_{\mathrm{c}} + \rho_{\mathrm{p}} h_i \tag{22}$$

$$\begin{aligned} D_{\mathrm{b}} = & \frac{E}{1-\nu^2} h_i \left(\frac{h_i^2}{12} + \alpha^2 d^2\right) \\ & + \mathcal{C}^{\mathrm{E}}_{11_{\mathrm{p}}} h_{\mathrm{c}} \left(\frac{h_{\mathrm{c}}^2}{12} + (1+\alpha)^2 d^2\right). \end{aligned} \tag{23}$$

Moreover a new term κ appears, which characterizes electromechanical conversion, as it comes as a factor of strains S_1 and S_2 produced by component E_3 of the electric field

$$\kappa = e_{13_{\mathrm{p}}}(1+\alpha)\frac{h_i + h_{\mathrm{c}}}{2} h_{\mathrm{c}}. \tag{24}$$

Physically, coefficient κ, expressed in Nm/V (or in C), quantifies the ability of the bimorph to transform voltage V_0 into a bending moment M_{E}.

3.3.2 Mechanical equations

In order to find the equations of the piezoelectric bimorph, the Hamilton principle is applied. The model thus obtained is close to that of plate equations with some adapted elements of reduction. However some extra terms appear which reflect the influence of a mechanical charge induced by the application of the electric field. The equation of dynamic equilibrium under external-load free condition is given by:

$$M_{\mathrm{b}}\ddot{w} + D_{\mathrm{b}}\Delta^2 w + \Delta\kappa E_3 = 0. \tag{25}$$

Moreover, the application of Hamilton's principle allows us to define boundary conditions along the curve Γ bounding the material domain:

$$K_{\mathrm{n}} + \kappa E_{3,n} = 0 \text{ or } \delta w = 0 \tag{26a}$$

$$M_{nn} + \kappa E_3 = \text{ or } \delta w_{,n} = 0 \tag{26b}$$

with K_{n} and M_{nn}, being respectively Kirschoff's shearing force and the bending moment according to the normal direction in a local coordinates system along Γ (*cf.* Fig. 2). Equation (25) shows that in the case of a non-uniform polarization, electromechanical conversion appears as a distributed mechanical load, while as shown by equations (26a, 26b), moments ($M_{\mathrm{E}} = \kappa E_3$) and shearing forces ($M_{\mathrm{E},n}$) appear along the boundary of the bimorph. This therefore ascertains that the model allows the phenomenon of the electromechanical coupling to be described at a macroscopic scale, starting from a local modelling.

3.3.3 Electrical equations

Modeling of the electric field already includes boundary conditions since they are linked to the voltage applied by the generators in (12). One can easily verify that such an approximation is a third order approximation if a fully electroded ceramic is considered. This leads to a uniform electric field since the influence of curving is neglected. In order to take into account a more accurate modeling, asymptotic developments of Φ and u_3 respectively to the third and second order would have been necessary [11].

The influence of those extra terms, however, is small. Indeed, as long as the thickness of the ceramic is small compared to that of the neutral material, the strain gradient according to the thickness is negligible in relation to its mean value, which means that the ceramic practically works under axial strain conditions.

In actual fact, the assumption of a uniform electrical field does not allow the electrical displacement field to be strictly conservative, that condition being respected within a second order precision. The application of the variational principal does not introduce any new element, and we have the following relation (27):

$$D_3 = -x_3 e_{13_{\mathrm{p}}}\Delta w - \epsilon^{\mathrm{S}}_{33_{\mathrm{p}}} E_3. \tag{27}$$

3.4 Resolution of the mechanical equation

According to the model obtained, the influence of the voltage supply is reduced to the creation of a mechanical charge induced by piezoelectric conversion. The nature of the problem is then not deeply modified compared with a problem in pure mechanics, so modal decomposition methods can be used [8,9].

Once natural pulsations and shapes of the structure are known, a modal base can be built with the normalized natural shapes $w_i(x_k) = \mu_i W_i(x_k)$ (μ_i: normalizing factor).

As each mode vector is normal to any other of the modal basis, we can calculate the response since, after exploiting this property, (25) comes to the resolution of a multitude of uncoupled differential equations defining normal coordinates $\eta_i(t)$:

$$\ddot{\eta}_i + \omega_i^2 \eta_i = \phi_i + \psi_i \tag{28}$$

$\phi_i(t)$ and $\psi_i(t)$ respectively represent the factor of participation of the distributed loads and the loads applied to the boundaries of the bimorph. In the case of the bimorph subjected only to the piezoelectric effect and starting from inactivated state, the mechanical response of the device is then:

$$w(x_k, t) = \sum_{i=1}^{\infty} \eta_i(t) w_i(x_k). \tag{29}$$

By introducing Laplace's transform $F_i(s)$ to describe the dynamic aspect which appears on the left side of equation (28) we get:

$$w(x_k, p) = -\sum_{i=1}^{\infty} \left[w_i(x_k) F_i(s) \int_{\Sigma} M_{\mathrm{E}}(s) \Delta w_i(x_k) \mathrm{d}\Sigma \right]. \tag{30}$$

4 Exploitation of the model

4.1 Synthesis of an equivalent electrical scheme

As the piezoelectric effect is reversible, as shown by equations (4a, 4b), the mechanical effects influence the electric values. Thus in our model, the electric field is "rigidly" imposed, and only **D** is sensitive to the deformation of the substrate. The field of electric displacement is only approximated to the second order, which implies that our model can not strictly verify the equality of total loads (in absolute value) on the two electrodes. However a good

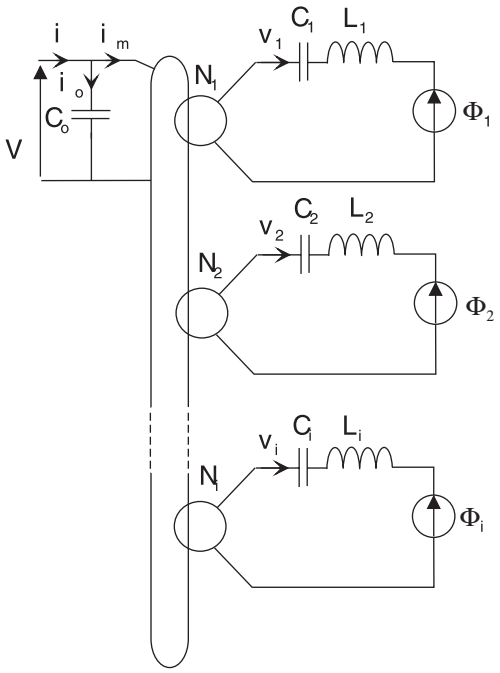

Fig. 4. Piezoelectric bimorph electrical equivalent scheme.

approximation of that load will be obtained by calculating the mean value of the loads on each electrode as in (31)

$$\overline{D_3} = (1+\alpha) d e_{13_\mathrm{p}} \Delta w - \epsilon^{\mathrm{E}}_{33_\mathrm{p}} E_3 = \frac{\kappa}{h_\mathrm{c}} \Delta w - \epsilon^{\mathrm{E}}_{33_\mathrm{p}} E_3. \quad (31)$$

By integrating $\overline{D_3}$ on Σ, we find the total load Q, which allows us to obtain the current in relation to the electric field. Then, by putting back (30, 7) in (31), we are able to find the admittance:

$$Y(s) = \sum_{i=0}^{\infty} \left[\left(\int_\Sigma \frac{\kappa}{h_\mathrm{c}} \Delta w_i(x_i) \mathrm{d}\Sigma \right)^2 F_i(s) \right] + C_0 s. \quad (32)$$

In formula (32) two distinct contributions emerge: on one hand the image of the dynamic effects with superposition of the different excited modes, and on the other hand the capacitive effect of the dielectric medium through the emergence of capacitance C_0, defined by:

$$C_0 = \epsilon^{\mathrm{E}}_{33_\mathrm{p}} \frac{S_\mathrm{c}}{h_\mathrm{c}} \cdot \quad (33)$$

The form of formula (32) reveals an electric scheme including capacitor C_0 parallel to an electrical dipole which corresponds to the transfer function $F_i(s)$ amplified by an electromechanical transformer.

The latter may temporally ignored if one is concerned with a purely electric equivalent circuit. Here, since we have ignored the dissipative effects, $F_i(s)$ corresponds to a second order with no damping, and we will then have a circuit including an infinite number of L_i, C_i series circuits wired in parallel with capacitor C_0 (Fig. 4). Thus, by calling A_i those factors which multiply function $F_i(s)$ in (32), the components are given by:

$$L_i = \frac{1}{A_i} \text{ and } C_i = \frac{A_i}{\omega_i^2} \cdot \quad (34)$$

The components can also be calculated as mechanical elements at the transformer secondary winding:

$$\begin{aligned} l_i &= \frac{1}{\mu_i^2} && \text{(kg)}, \\ c_i &= \frac{\mu_i^2}{\omega_i^2} && \text{(m/N)}, \\ N_i &= \int_\Sigma \frac{\kappa}{h_\mathrm{c}} \Delta W_i(x_{k0}) \mathrm{d}\Sigma && \text{(C/m or N/V)}. \end{aligned} \quad (35)$$

Those relations show that inductance L_i is an image of the vibrating mass and capacitance C_i is linked to the compliance of the ith mode. It can also be noticed that those characteristics depend a good deal on the mode shape of the warped bimorph through the electromechanical transformation coefficient as relation (35) shows. This makes the design of the transducer rather complicated, for we have to know the resonance frequencies and the associated shapes.

Our next step will concern the influence of a mechanical load $p(x_k, t)$ applied on the stator surface, deriving from an external potential. Its influence on the flexure will not be dealt with any differently from that of the original piezoelectric load induced in the bimorph. We will then calculate a factor of participation ϕ_{i_p} of the load for each mode which is added to the terms on the right side of equality in equation (28). The mechanicals loads are represented on an electric scheme as voltage sources in series with the element in the equivalent scheme, the corresponding tensions being given by $N_i \phi_{i_\mathrm{p}}$ (Fig. 4).

4.2 Application to the stator of a travelling wave motor

In order to validate the model thus obtained, the previous formulas will now be used for a practical application. An interesting one is the travelling wave motors which are currently among the most effective piezoelectric actuators. Moreover since this application exploits the mechanical resonance phenomenon, one of the secondary circuits in Figure 4 can be select. This equivalent scheme is cumbersome to use otherwise. The modelized stator is simply constituted by a ring-shaped bimorph the inside side of which is linked to the hub *via* an equally ring-shaped veil of thin metal. This design entails a degenerescence in the flexing modes in the orthoradial direction, making it possible to induce a progressive wave.

The latter is created by energizing both modes simultaneously *via* two sets of ceramics laid out in spacial quadrature, properly polarized, and separately powered by a diphased power source [12].

The chosen lay-out requires two distinct domains to be considered, the decoupling veil and the track. Although the veil is not active, equations (25, 26a, 26b) remain valid since the veil may be considered as a bimorph with no active part: we are then back to the classical equations of the plates.

The final step consists in ensuring continuity between both domains, while keeping the previous method. To do so we will resort to Lagrange multipliers which, allow complementary boundary conditions to be defined, while imposing the conditions of kinematic continuity between the two sub domains. Here, we make the assumption that the veil and the track are perfectly clamped, which is expressed on the common boundary $\Gamma_{t\cap v}$ by (t and v representing respectively the values of the track and the veil):

$$w_v = w_t \quad \text{and} \quad w_{v,n} = w_{t,n}. \tag{36}$$

The application of the Hamilton principle to the augmented Lagrangian makes it possible to determine further conditions expressing the action and reaction principle along $\Gamma_{t\cap v}$:

$$\begin{aligned} K_{n_v} + K_{n_t} + M_{\mathrm{E},n} &= 0 \\ \text{and} \quad M_{nn_v} + M_{nn_t} + M_{\mathrm{E}} &= 0. \end{aligned} \tag{37}$$

5 Experimental validation

5.1 Experimental lay-out

In order to allow experimental assessment a bench adapted to the problems of identification of the electromechanical parameters of electro-active transducers has been developed. The different elements of the bench are shown in Figure 5. The lay-out is set up around a signal analyzer (HP 3562A) which allows the calculation of admittances and vibratory gain transfer functions. It also generates a variable amplitude signal (0−5 V) with a low distortion rate, over a large frequency range (0−100 kHz). In order to generate systems of diphased voltage, the signal is processed by an analogical phase-shifting device, then amplified by a wide-band power device (0−150 kHz) with automatic gain control.

This whole device allows the independent control of the amplitudes and phases of the different tracks. As for the measures of electrical values, they are done through voltage probes and directly processed by the analyzer. The measures of the current are achieved through shunts which are better adapted than Hall effect probes for such levels and frequencies, in particular for measuring phases.

For a complete characterization the bench also has a laser interferometer to measure vibrating speed and amplitudes accurately and without interference since there is no contact. It allows the acquisition of amplitude and phase distribution in each natural mode, and identification of electromechanical conversion parameters. Finally the coordination and programming of identification procedures are monitored by a computer linked to the different devices *via* a GPIB connection.

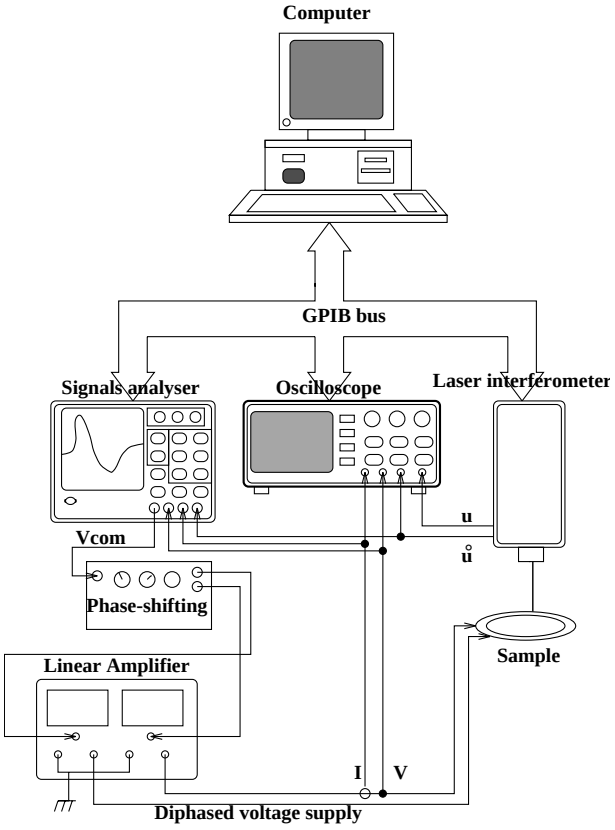

Fig. 5. Electroactive transducer characterization bench.

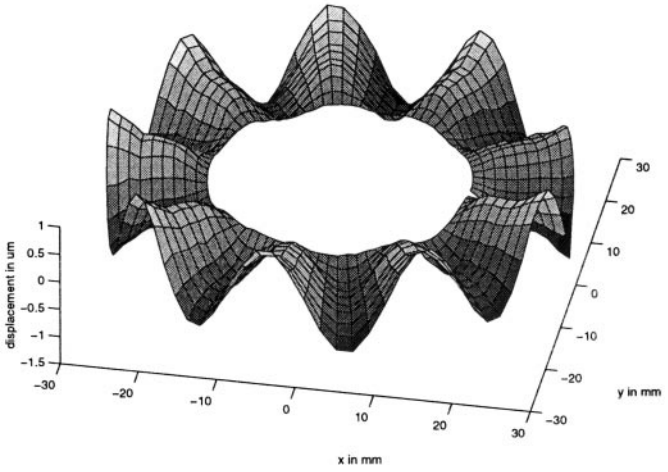

Fig. 6. Laser cartography of the studied stator ($n = 9$).

The method used to identify the components of the equivalent scheme for a given mode is that of quadrantal frequency, as it guarantees weak sensitivity for the non-linearities which have to be dealt with.

Table 1. Comparison of theoretical and practical results (9th mode).

	theory	measures
f_9 (kHz)	40,7	39,6
L_9 (mH)	36	34
C_9 (pF)	429	467
R_9 (Ω)	*67*	*64*
N_9 (C/m ou N/V)	1.17	1.15
C_0 (nF)	14.5	13.7
k_9 (%)	18	16

Table 2. Comparison of theoretical and practical results (10th mode).

	theory	measures
f_{10} (kHz)	51.1	47.7
L_{10} (mH)	112	98
C_{10} (pF)	86	113
R_{10} (Ω)	*82*	*72*
N_{10} (C/m ou N/V)	0.94	0.96
C_0 (nF)	14.5	14.2
k_{10} (%)	4.5	7.8

5.2 Experimental results

The theoretical developments described above have been applied to an USR60 travelling-wave motor stator modified in view of obtaining a new type of actuator. The change brought to the original device consists in suppressing the teeth, which responds to the geometrical assumptions of the modelization. The electrical and mechanical values of the model have been calculated from a computerized implementation, taking into account a tensorial characterization of hard ceramics (type P1-89) with value d_{31} slightly modified. Particular attention has been paid to the study of rank 9 mode for which the stator is designed and for which resonance is significant. This makes measurement all the more reliable. Mode 10 has also been identified.

Moreover, trials have been made under reduced sinusoidal voltage (40 V_{pp}) to avoid amplitudes which might damage the ceramics.

Results for both methods are summed up in Tables 1 and 2. The presence of a resistance (R_9 and R_{10}) which evaluates mechanical losses will be noted. This has been made possible by introducing a damping term in $F_i(s)$ transfer function. Such a term however is not known *a priori* and should be adjusted through identification, or be empirically evaluated by choosing $1\times10^{-3} \leq \xi \leq 1\times10^{-2}$.

As far as electric values are concerned, theoretical results are close to experimental measures, in spite of the significant assumptions made concerning the electric field. It remains to be determined whether the adjustment of coefficient d_{31} is really due to the fact that actual ceramics are slightly different from the material originally considered, or whether it is a consequence of some non-linear effects ignored in the model.

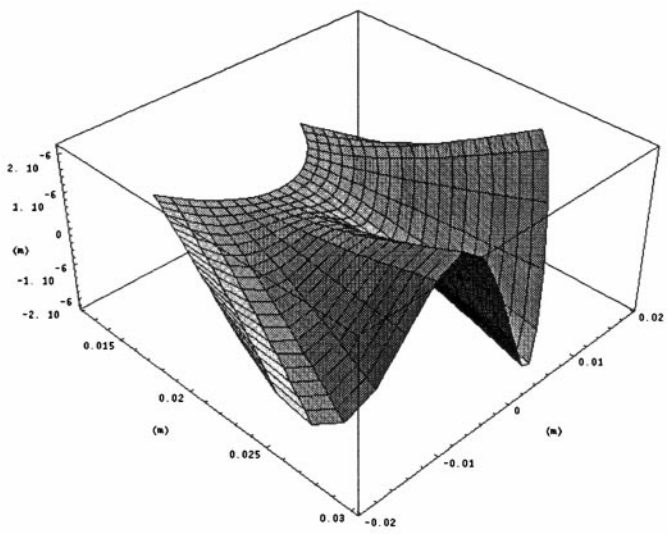

Fig. 7. Theoretical displacement of the neutral plane (two wavelengths represented).

The mechanical aspect is also correctly described since the deformed shapes which have been measured and those which have been calculated (*cf.* Figs. 6 and 7) coincide, particularly with respect to amplitudes. The resonance frequency is relatively well-determined, but it is to be noted that for low deformation amplitudes the frequential shift due to non-linearities remains relatively weak [13].

6 Conclusion

The method implemented is particular in that it systematically modelizes the electromechanical conversion which occurs in bimorph structures, by natural integration of the physical aspects of the materials and the geometry of the actuator. Considering the results, the model described seems satisfactory, at least in the experimental conditions exposed. Further investigations need to be made to determine the influence of non-linearities inherent to ceramics, particularly when the ceramics are fed with large voltages.

Furthermore, the model is necessarily limited in frequency since, from the first, the influence of shearing stresses have been neglected. This was useless in the case of the stator studied. Indeed, even for a ninth rank mode, the ratio between the wavelengths and the thickness of the device is large.

Moreover, the model describes bimorph devices which evolve in a dynamic way. This model is originally more orientated towards a description of actuators which work near resonance frequencies. However, it can easily be extrapolated to actuators working in quasistatic operation. The only difference will occur during resolution, as it will be pointless to go through modal analysis.

In the long term, the proposed modelling method seems to be a strong basis for solving the optimal design problems of piezoelectric actuators, considering in particular the generic property of the energetic formulation used. Furthermore, the direct connection of the developed model with equivalent circuit representations should allow the integration of the power supply circuit into the global design procedure.

References

1. E. Piécourt, B. Nogarède, J. Phys. III France **5**, 689 (1995).
2. B. Nogarède, Techn. Ing. D3765 (1996).
3. T. Ikeda, *Fundamentals of piezoelectricity* (Oxford Science Publications, 1990), pp. 3–30.
4. C. Lanczos, *Variational principles of mechanics* (Dover Publications, 1970), pp. 3–73.
5. L. Landau, E. Lifchitz, *Physique théorique,* tome 1: Mécanique (Mir, 1990), pp. 29–41.
6. P. Hammond, *Energy Methods in Electromagnetism* (Oxford Science Publications, 1981), pp. 25–113.
7. L. Landau, E. Lifchitz, *Physique théorique,* tome 7: Théorie de l'élasticité (Mir, 1990), pp. 8–45.
8. M. Géradin, D. Rixen, *Théorie des vibrations: application à la dynamique des structures* (Masson, 1996), pp. 158–167.
9. L. Meirovitch, *Element of vibration analysis*, 2nd edn. (McGraw-Hill International Edition, 1986), pp. 205–244.
10. P. Moon, D.E Spencer, *Field theory handbook*, 2nd edn. (Springer-Verlag, 1971).
11. H.F. Tiersten, *Equations for the extension and flexure of relatively thin electroelastic plates undergoing large electric fields*, AMD-Vol. 161/MD-Vol42, Mechanics of Electromagnetic Materials Ans Structures (ASME 1993), pp. 21–34.
12. S. Ueha, Y. Tomikawa, *Ultrasonics motors: theory and applications* (Oxford Science Publications, 1993), pp. 8–25.
13. N. Aurelle, D. Guyomard, P. Gonnard, L. Eyraud, *Non linear behavior of ultrasonic transducers*, Ultrasonic International, 4-7 July 1995.